

**Effect of heat treatment on mechanical properties and corrosion resistance of Nickel Alloy
UNS N07718 – 140 ksi and 150 ksi grades**

Julia Rosenberg
VDM Metals International GmbH
Kleffstrasse 23
58762 Altena, Germany

Jutta Klöwer
VDM Metals International GmbH
Kleffstrasse 23
58762 Altena, Germany

John Groth
VDM Metals USA, LLC
14255 Mt. Bismark St.
Reno, NV 89506, USA

Christoph Bosch
Salzgitter Mannesmann Forschung GmbH
Ehinger Strasse 200
47259 Duisburg
Germany

Georgi Genchev
Salzgitter Mannesmann Forschung GmbH
Ehinger Strasse 200
47259 Duisburg
Germany

ABSTRACT

UNS⁽¹⁾ N07718 is one of the most commonly used alloys in the oil and gas industry. The chemistry of the precipitation hardenable nickel-chromium-iron alloy is characterized by additions of niobium and molybdenum as well as certain amounts of aluminum and titanium, resulting in excellent corrosion resistance in oil and gas applications and high strength properties.

Based on the API⁽²⁾ Standard 6ACRA¹ the alloy is available in two grades (min. yield strength 120 ksi and 140 ksi). Due to a strong interest in the market to have a grade with higher strength, the development of a third, 150 ksi grade was started. It is well known that the heat treatment of an alloy can have significant effects on the microstructure, mechanical properties as well as corrosion resistance. To study the effect of the heat treatment and the resultant properties of the alloy an intensive testing program of all three grades (120 ksi, 140 ksi and 150 ksi) was launched. In addition to the microstructure and mechanical properties a variety of corrosion tests were performed. The different mechanisms of environmental cracking were considered by using several test methods. Sulfide stress cracking (SSC) and galvanically induced hydrogen stress cracking (GHSC) tests were performed according to NACE⁽³⁾ TM0177-2016 Method A.²

(1) Unified Numbering System for Metals and Alloys (UNS), SAE International, Warrendale, PA

(2) American Petroleum Institute (API), 1220 L St., N.W., Washington, D.C. 20005-4070

(3) National Association of Corrosion Engineers (NACE) International, 15835 Park Ten Place, Houston, TX 77084

Stress corrosion cracking (SCC) resistance was investigated using C-ring tests according to NACE TM0177 Method C at Level VI/VII (NACE MR0175/ISO 15156-3, Table E.1)³ for 3 and 6 months. Slow strain rate (SSR) tests under cathodic polarization were performed to study the resistance to hydrogen embrittlement (HE).

In terms of resistance to corrosion and hydrogen embrittlement the 150 ksi grade of UNS N07718 was found to perform equally well or even better than the lower strength grades.

Key words: UNS N07718, Sulfide stress cracking (SSC), Stress corrosion cracking (SCC), Hydrogen embrittlement, 140 and 150 ksi grade.

INTRODUCTION

For the application of materials in the oil and gas exploration it is necessary to select suitable alloys very carefully. The environmental and operating conditions are very harsh and the material has to meet several different requirements at the same time.

High pressures and temperatures coupled with the presence of hydrogen sulfide and chlorides create challenging demands on the materials.⁴ NACE MR0175/ ISO⁽⁴⁾ 15156-3 gives an overview of all approved materials in consideration of the environmental conditions.^{2, 5}

Beside the corrosion resistance of the materials, the mechanical properties play also an important role. In recent years, the interest in the O&G industry for using higher strength materials increased. Due to a number of reported failures of Nickel alloys with high strength, the resistance to Hydrogen Stress Cracking and Hydrogen Embrittlement raised more and more attention.⁶

Nickel base alloy UNS N07718 is a precipitation hardenable material, which is used for many years in the oil and gas exploration. It has outstanding mechanical properties and excellent corrosion resistance in the presence of hydrogen sulfide and carbon dioxide.^{4, 7} The great properties are a result of the microstructure, consisting of matrix γ , precipitates γ'' , γ' , δ and carbides. Gamma double prime (Ni_3Nb) is the main strengthening phase in this alloy.⁸⁻¹¹

In the last years, several investigations regarding HE were performed and the effect of the different precipitation phases like gamma', gamma'' and delta phase were considered more closely.^{6, 11-19}

These results showed that the HE sensitivity was low when gamma'' and delta phase were dissolved.¹² In other words, increased strength has been correlated with increased hydrogen embrittlement susceptibility.^{6, 19, 20}

B. Kagay et al summarized data from several studies about HE of different Ni-base alloys. Under consideration that the testing parameters of the performed SSR hydrogen embrittlement studies like solution, temperature and strain rate were different, there was no clear trend between HE susceptibility and strength levels. Comparison of the test results of an over-aged sample and an under-aged sample of Alloy UNS N07718 showed that the ratio of elongation for the over-aged condition were inferior compared to the under-aged condition even when the strength was on the same level. There was a wide range of studies with different outcomes about the effects on hydrogen embrittlement and some look like contradictory. The majority of the studies showed more or less clear that the HE susceptibility is affected by grain boundary precipitation and γ'' and γ' volume fraction and/or size.¹⁹ The strength is not the decisive reason for HE susceptibility as claimed in previous works, it is more the microstructure and precipitating behavior which has, in turn, an effect on the strength. The aim of this study is to show the effect of different heat treatments, more specifically the effect of different strength/hardness grades on the microstructure, the corrosion resistance and HE susceptibility of alloy UNS N07718.

(4) International Organization for Standardization (ISO), 7 ch. De la Voie-Creuse, Case Postale 56, Geneva, Switzerland

EXPERIMENTAL PROCEDURE

Material

For the investigation program, double-melt ingots (VIM (Vacuum Induction Melting) + VAR (Vacuum Arc Remelting)) of three separately processed heats designated A, B and C, with nominal chemical composition shown in **Table 1** were produced. The ingots were homogenized and hot forged to round bars with a diameter of 203.2 mm (8 inch). The round bars were furnace heat treated according to **Table 2**. For this, all samples were solution annealed at 1032 °C (1890 °F). Consequently, single-step age hardening for the 120 ksi (A1 / B1 / C1) and 140 ksi (A2 / B2 / C2) grades, and two-step age hardening for the 150 ksi (A3 / B3 / C3) grade, respectively, were conducted.

Table 1
Chemical composition of Alloy UNS N07718 in percentage mass fraction

Element	Sample designation									NACE MR 0175 / ISO 15156-3:2015 requirements	
	A1	A2	A3	B1	B2	B3	C1	C2	C3	min	max
Ni	54.09	54.4	54.06	54.39	53.84	54.69	54.33	54.35	54.25	50.0	55.0
Cr	18.51	18.46	18.52	18.61	18.59	18.55	18.46	18.44	18.46	17.0	21.0
Fe	17.53	17.23	17.54	17.25	17.84	16.97	17.48	17.49	17.58		bal.
Nb	4.97	4.99	4.98	4.98	4.94	5.00	4.99	5.00	4.99	4.75	5.50
Mn	0.04	0.04	0.04	0.03	0.04	0.03	0.02	0.02	0.02		0.35
Si	0.05	0.05	0.04	0.08	0.09	0.08	0.06	0.06	0.06		0.35
Mo	3.11	3.12	3.12	3.05	3.03	3.07	3.04	3.04	3.03	2.8	3.3
Ti	1.01	1.02	1.01	0.94	0.93	0.96	0.95	0.95	0.94	0.65	1.15
P	0.004	0.004	0.004	0.005	0.005	0.005	0.004	0.005	0.004		0.015
Al	0.55	0.55	0.55	0.51	0.54	0.47	0.54	0.52	0.54	0.20	0.80
C	0.009	0.011	0.010	0.012	0.012	0.014	0.013	0.011	0.013		0.08
Co	0.05	0.05	0.05	0.06	0.05	0.06	0.04	0.04	0.04		1.0
B	0.004	0.004	0.004	0.004	0.004	0.004	0.004	0.004	0.004		0.006
S	0.0008	0.0010	0.0010	<0.0005	0.0006	0.0005	<0.0005	<0.0005	0.0006		0.015

Table 2
Parameters for the heat treatment performed on Alloy UNS N07718

Sample designation	Material grade	Heat treatment					
		Solution annealing					
		Temperature	Holding time	Cooling rate	Temperature	Holding time	Cooling media
All	All	1032 °C	1 – 2 h	-	-	-	Air

		Age hardening					
		Temperature	Holding time	Cooling rate	Temperature	Holding time	Cooling media
A1 / B1 / C1	120 ksi	790 °C	7 – 8 h	-	-	-	Air
A2 / B2 / C2	140 ksi	760 °C	8 h	-	-	-	Air
A3 / B3 / C3	150 ksi	720 °C	8 h	50 °C / h	620 °C	8 h	Air

*The temperatures were monitored by using heat sinks with similar diameter (+/- 5mm) and thermocouples.

Metallography and Mechanical Testing

Microstructure

Microstructural investigations were performed on mechanically polished and chemically etched specimens. For etching, a pickling solution containing 100 mL H₂O, 100 mL HCl, and 10 mL HNO₃ was used. Evaluation of the microstructure was performed using light optical and scanning electron microscopy techniques. The grain sizes were measured using the concentric circles method in accordance with ASTM⁽⁵⁾ E112²¹.

Tensile Testing

Tensile testing was conducted according to ISO 6892-1²² for room temperature and -2²³ for testing at elevated temperatures. Smooth specimens in longitudinal or transverse direction were machined and tested at room temperature, 175 °C (347 °F), and 205 °C (401 °F).

Charpy Impact Testing

Charpy specimens with the notch in longitudinal or transverse direction were tested at a temperature of - 60 °C (- 76 °F) according to ISO 148-1²⁴.

Hardness

Rockwell hardness (HRC) test were performed according to ISO 6508-1²⁵ in three different positions of the material: approximately 2.54 mm (0.1 inch) below surface, at mid-radius and at center. Three indentations were performed per position.

Corrosion Testing

The corrosion testing program was established to meet the requirements of NACE MR0175 / ISO15156-3³ for qualification of CRAs for H₂S-service, taking SSC, SCC and GHSC into account. Additionally, SSRT testing was performed to determine the susceptibility to hydrogen embrittlement.

Sulfide Stress Cracking (SSC) Resistance

SSC testing using NACE TM0177 Method A² was performed at 24 °C ± 3 °C (75 °F ± 5 °F) on triplicate smooth round specimens with a gauge diameter of 6.35 mm (0.25 inch) and a gauge length of 25.4 mm (1 inch). The testing was carried out in Solution A saturated with 100 kPa (14.5 psi) H₂S, resulting in an

⁽⁵⁾ American Society for Testing and Materials (ASTM) International, 100 Barr Harbor Drive, West Conshohocken, PA, 19428

initial pH of 2.7; the final pH was measured to be less than 4.0. Stress level of 90 % AYS was applied by deflection of the proof ring. Test duration was 720 h (30 d).

Galvanically Induced Hydrogen Stress Cracking (GHSC) Resistance

GHSC testing was performed in accordance with the previously stated conditions for SSC testing. In addition, the tested specimens were electrically coupled by platinum wire to carbon steel, which was fully immersed in the test solution.

Stress Corrosion Cracking (SCC) Resistance

SCC testing was performed using NACE TM0177 Method C (C-ring test)². The material was tested under Level VI and Level VII conditions, respectively, as specified by NACE MR0175 / ISO 15156-3³, Table E.1. For all grades of Alloy 718, SCC testing was conducted on triplicate C-ring specimens at 100 % of AYS at the test temperature. For each material grade, four C-ring specimens were machined in the transverse orientation with the apex at the mid-radius location. The C-ring dimensions were: 40 mm (1.57 inch) outer diameter (OD) x 4 mm (0.16 inch) wall thickness (WT) x 15 mm (0.59 inch) width (W). For each set of four specimens, one C-ring was strain gauged in order to determine the necessary deflection corresponding to 100 % AYS at test temperature. The determined data was then utilized to deflect the tested triplicate set of specimens. SCC testing was carried out in 15 L autoclaves made of corrosion resistant material. After placing the specimens in the vessel, approximately 10 L of the test solution was added, so that all specimens were completely immersed in the liquid phase resulting in a solution volume to surface area ratio of about 35 mL/cm². Temperature was daily monitored and varied no more than ± 2 °C (4 °F) for Level VI and ± 3 °C (5 °F) for Level VII condition, respectively. Separate specimens were used for 3 months testing at Level VI and VII and 6 months testing at Level VII. After exposure to the corrosive environment, C-ring specimens were rinsed with distilled water and photographed. Examination for evidence of cracking was performed visually at 10x magnification.

Hydrogen Embrittlement (HE) Resistance

Slow Strain Rate Tensile (SSRT) tests were used to determine the susceptibility to HE of the tested materials. Standard SSRT test specimens according to NACE TM0198-2016²⁶ with gauge section diameter of 3.81 mm (0.15 inch) and gauge section length of 25.4 mm (1 inch) were used. The tests were performed at 40 °C (104 °F). For each material, two specimens were tested in control environment (distilled water purged with nitrogen) and three specimens in test environment (0.5 M sulfuric acid solution and applied cathodic current density of 5 mA cm⁻². The strain rate was 1×10^{-6} s⁻¹ (cross-head speed: 2.5×10^{-5} mm s⁻¹).²⁷ Time-to-failure, reduction-in-area and elongation at failure are reported. After test end, all specimens were inspected under a microscope at 20x magnification in order to determine the occurrence of secondary cracking.

RESULTS AND DISCUSSION

Microstructure

Typical microstructures of Alloy 718 in the different age-hardened conditions are depicted in **Figure 1**. The microstructure was found to consist of an austenitic matrix with an equiaxed grain structure and a unimodal grain size distribution. The average grain size according to ASTM E112²¹ was found to be No. 4 or finer. SEM micrographs of etched specimens in the different age-hardened conditions are shown in **Figure 2**. White needle-like precipitates on the grain boundary were identified as δ phase, while tiny particles in the matrix could be assigned to the γ' and metastable γ'' phases. Decreasing the age hardening temperature leads to γ'' particles of smaller size, which were found to be responsible for the strength increase in these materials.

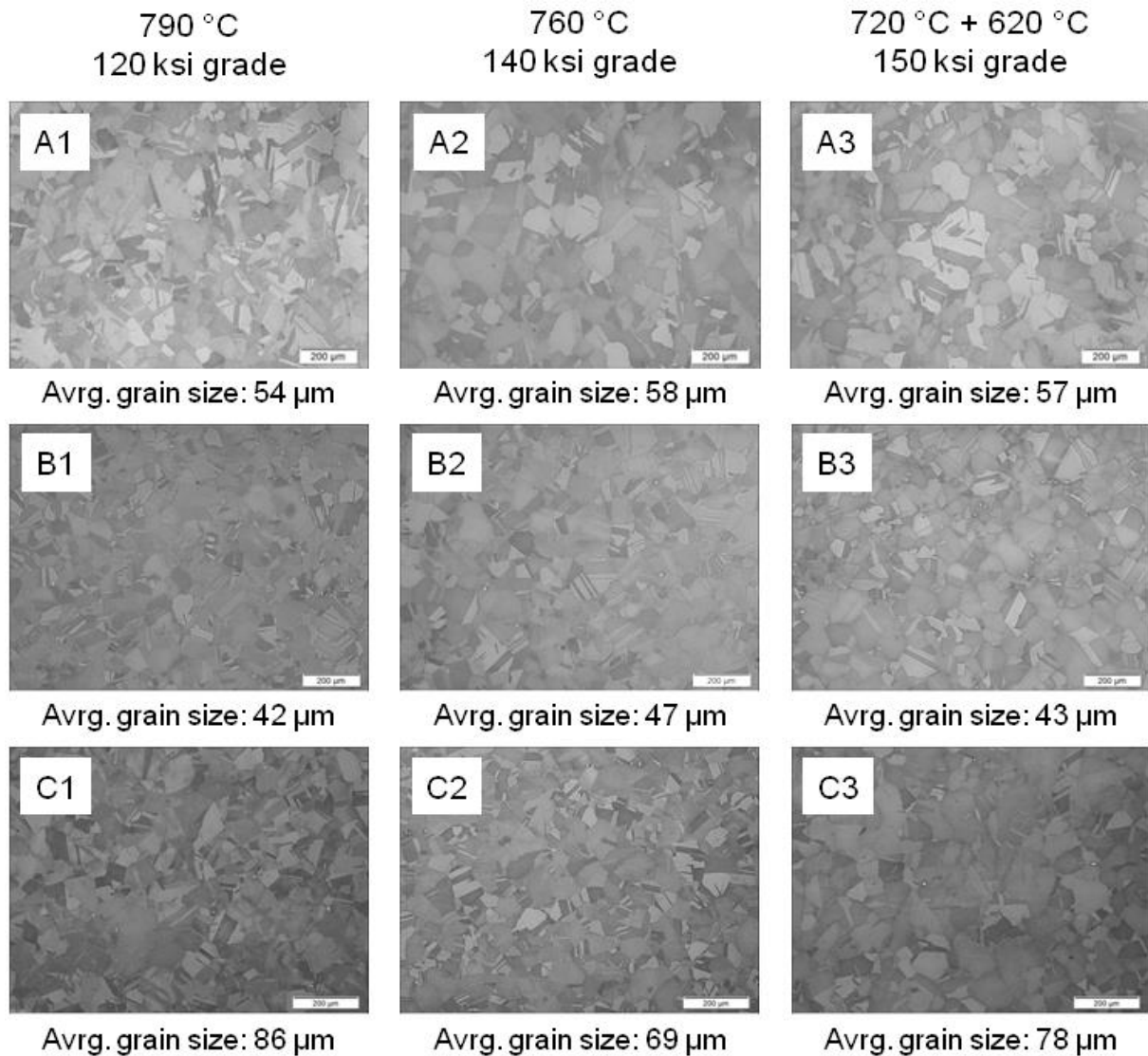


Figure 1: Typical microstructure of Alloy 718 in the different age-hardened conditions at 100x magnification. Average grain sizes were determined according to ASTM E112. For etching V2A was used.

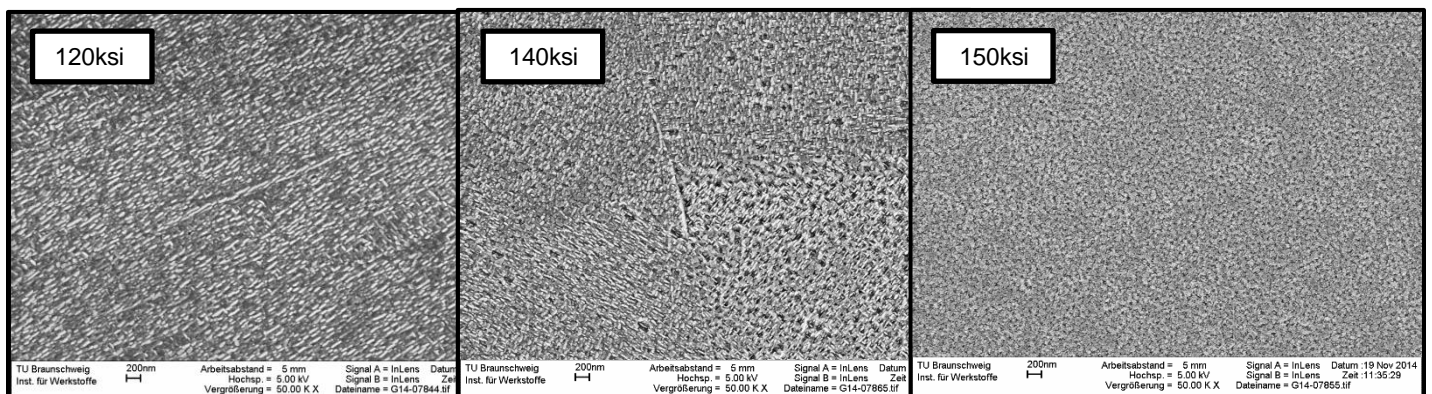


Figure 2: SEM micrographs of samples 120ksi (age hardened at 790 °C), 140ksi (age hardened at 760 °C) and 150ksi (double-step age hardened at 720 °C / 620 °C). All specimens etched using V2A; magnification = 50,000X. The γ' -particles are point-type while the γ'' particles have a line shape.

Mechanical Properties

Alloy UNS N07718 was successfully produced in three different strength classes with minimum yield strengths of 827 MPa (120 ksi), 965 MPa (140 ksi), and 1034 MPa (150 ksi). Typical mechanical properties of Alloy UNS N07718 in the different material grades are provided in **Table 3**. The yield strengths are found to be well above the specified minimum for the corresponding grades. For the 120 ksi and 140 ksi grades of Alloy UNS N07718, ductility parameters (elongation and reduction of area) are within the requirements of API 6ACRA and API 5CRA specifications for precipitation hardened nickel base alloys. Additionally, tensile testing was performed at elevated temperatures of 175 °C (347 °F) and 205 °C (401 °F) with the results given in **Table 4**. Good toughness properties were determined for all three material grades of Alloy UNS N07718 tested here (Table 5). The hardness of all nine materials is shown in **Table 6**. A linear relationship between hardness and AYS resp. SMYS was found for Alloy UNS N07718 (**Figure 3**). Thus, increasing yield strength for Alloy UNS N07718 leads to an increase of the measured hardness.

Table 3
Average mechanical properties of Alloy 718 evaluated at room temperature.

Sample des.	Material grade		Orientation	Tensile test parameters					
				R _{p0.2}		UTS		E	RoA
	ksi	MPa		L / T	MPa	ksi	MPa	ksi	%
A1	120	827	L	972	141	1285	186	28	49
			T	961	139	1274	185	24	32
A2	140	965	L	1051	152	1294	188	25	51
			T	1039	151	1289	187	26	39
A3	150	1034	L	1106	160	1294	188	23	54
			T	1116	162	1301	189	19	38
B1	120	827	L	930	135	1248	181	28	49
			T	933	135	1245	181	25	35
B2	140	965	L	1048	152	1277	185	26	49
			T	1042	151	1281	186	23	38
B3	150	1034	L	1106	160	1292	187	24	53
			T	1129	164	1312	190	17	43
C1	120	827	L	942	137	1252	182	27	48
			T	929	135	1246	181	25	38
C2	140	965	L	1031	150	1280	186	27	51
			T	1012	147	1275	185	23	39
C3	150	1034	L	1129	164	1324	192	24	52
			T	1157	168	1348	196	21	41

L: longitudinal; T: transverse; R_{p0.2}: 0.2 % offset yield strength; UTS: ultimate tensile strength; E: elongation; RoA: reduction of area

Table 4
Average tensile properties of Alloy 718 at elevated temperatures determined in transverse direction.

Sample des.	Material grade		175 °C						205 °C					
			R _{p0.2}		UTS		E	RoA	R _{p0.2}		UTS		E	RoA
	ksi	MPa	ksi	MPa	ksi	MPa	%	%	ksi	MPa	ksi	MPa	%	%
A1	120	827	132	908	178	1228	20	28	128	883	176	1216	22	32
A2	140	965	138	952	177	1223	22	36	138	953	178	1225	25	36
A3	150	1034	148	1019	178	1226	22	36	148	1019	177	1220	22	37
B1	120	827	126	867	172	1183	23	36	124	854	172	1183	25	35
B2	140	965	140	968	177	1220	25	39	140	966	177	1219	26	40
B3	150	1034	151	1044	180	1239	20	41	150	1034	179	1237	23	39
C1	120	827	129	890	174	1201	22	37	126	868	173	1196	25	37
C2	140	965	139	961	176	1214	22	39	138	952	177	1218	25	39
C3	150	1034	154	1059	181	1248	22	43	154	1063	182	1254	22	43

R_{p0.2}: 0.2 % offset yield strength; UTS: ultimate tensile strength; E: elongation; RoA: reduction of area

Table 5
Charpy V-notch impact testing results obtained for Alloy 718.

Sample designation	Material grade	Charpy Impact (-60°C)		Lateral Expansion	
		J		mm	
	ksi	L	T	L	T
A1	120	85	61	0.90	0.70
A2	140	107	63	1.10	0.70
A3	150	117	79	1.07	0.80
B1	120	113	73	0.82	0.55
B2	140	109	69	0.87	0.55
B3	150	126	88	0.98	0.62
C1	120	116	80	0.90	0.70
C2	140	117	79	0.93	0.67
C3	150	118	83	0.90	0.63

L: longitudinal orientation; T: transverse orientation (crack plane orientation: C-L)

Table 6
Average hardness (HRC) measured at different positions of the round bars

Sample des.	Material grade	Location of hardness (HRC) measurement			Min (single values)	Max (single values)
	ksi	surface*	mid-radius*	center**		
A1	120	37 / 38 / 39	37 / 36 / 37	36.7	36.0	40.0
A2	140	42 / 41 / 42	41 / 42 / 42	41.3	41.0	42.0
A3	150	43 / 43 / 45	43 / 44 / 45	42.7	42.0	45.0
B1	120	39 / 39 / 39	40 / 38 / 39	37.0	35.0	40.0
B2	140	42 / 41 / 41	41 / 42 / 41	41.0	40.0	42.0
B3	150	43 / 43 / 43	41 / 43 / 43	42.3	41.0	44.0
C1	120	37 / 37 / 37	37 / 37 / 37	36.4	36.0	38.2
C2	140	40 / 39 / 40	39 / 40 / 40	39.3	38.9	39.9
C3	150	42 / 42 / 42	43 / 43 / 43	41.9	41.4	42.8

*Average of 3 values at each direction (3 values from one location: 0°, 120°, 240°)

**Average of 3 values

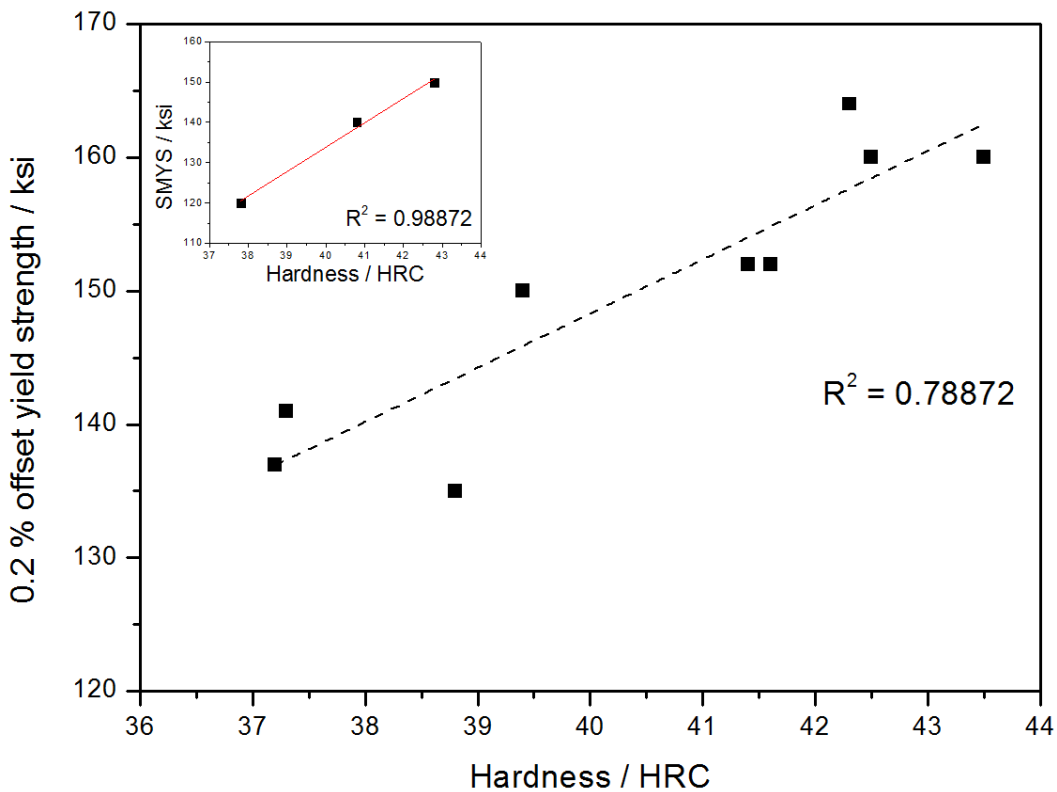


Figure 3: Correlation between yield strength ($R_{p0.2}$) and hardness (HRC) for Alloy 718. Inset: Correlation between specified minimum yield strength and hardness (HRC).

Corrosion Resistance

Corrosion testing was performed considering qualification requirements for SSC, GHSC, and SCC as given by NACE MR0175 / ISO 15156-3³. In case of precipitation-hardened nickel base alloys, both SCC and GHSC are stated as primary and SSC as secondary (possible) mechanisms. Moreover, special attention should be paid to nickel base alloys in the aged conditions as they contain secondary phases and can potentially suffer from HSC when galvanically coupled to carbon or low-alloy steel. An overview of the corrosion test environmental conditions is shown in **Table 7**.

Sulfide Stress Cracking (SSC) Resistance

SSC resistance of Alloy UNS N07718 was evaluated using uniaxial tensile tests as given by NACE TM0177 Method A². No cracking was found for any of the tested material grades of Alloy UNS N07718 for the test duration of 30 d (**Figure 4**).

Galvanically induced Hydrogen Stress Cracking (GHSC) Resistance

GHSC testing was conducted using the same conditions and specimen geometry as for SSC testing but with the GHSC test specimens coupled to carbon steel. In this way, a galvanic effect based on the different potentials of the metals is established and may lead to accelerated cracking of the tested CRA. However, in case of Alloy UNS N07718 tested here, no cracking was observed for the test duration of 30 d (**Figure 4**).

Stress Corrosion Cracking (SCC) Resistance

SCC resistance was evaluated using NACE TM0177 Method C². The tests were performed at environmental conditions corresponding to Level VI (90 d) and Level VII (90 d and 180 d) given by NACE MR0175 / ISO 15156-3³, Table E.1 (**Table 7**). For each tested grade of Alloy UNS N07718, three C-ring specimens were exposed after applying a stress corresponding to 100 % of AYS at the test temperature. After test end, all tested specimens were cleaned. No cracks or other relevant defects were found on the surfaces of the specimens upon stereomicroscope analysis (**Figure 4**). One series of C-Rings (6-months, Level VII) were investigated by using light optical microscopy techniques after the corrosion test.

Figure 5 shows micrographs of sample C3. There was no evidence of cracks or other relevant defects. The authors of the present paper are aware of a possible negative effect of elemental sulfur on the corrosion performance of CRAs. For this reason, a future work including SCC testing in the presence of S⁰ on alloy UNS N07718 is already being planned.

Table 7
Corrosion test environmental conditions for Alloy 718.

Cracking mechanism	Specimen type	Specimens per heat	Duration / d	T / °C	H ₂ S / kPa	CO ₂ / kPa	pH End	Cl ⁻ / mg L ⁻¹	S ⁰ / mg L ⁻¹	σ / % AYS	Galvanic coupling	Pass / Fail
SSC	*	3	30	24	100	-	2.8 / 3.0 / 3.0	Test Solution A***	-	90	no	P
GHSC	*	3	30	24	100	-	3.8 / 3.6 / 3.7		-	90	yes	P
SCC	**	3	90	175	3,500	3,500	-	139,000	-	100	no	P
	**	3	90	205	3,500	3,500	-	180,000	-	100	no	P
	**	3	180	205	3,500	3,500	-	180,000	-	100	no	P

* acc. NACE TM0177-2016 Method A (round bar tensile test specimen)

** acc. NACE TM0177-2016 Method C (C-ring specimen)

*** acc. NACE TM0177-2016

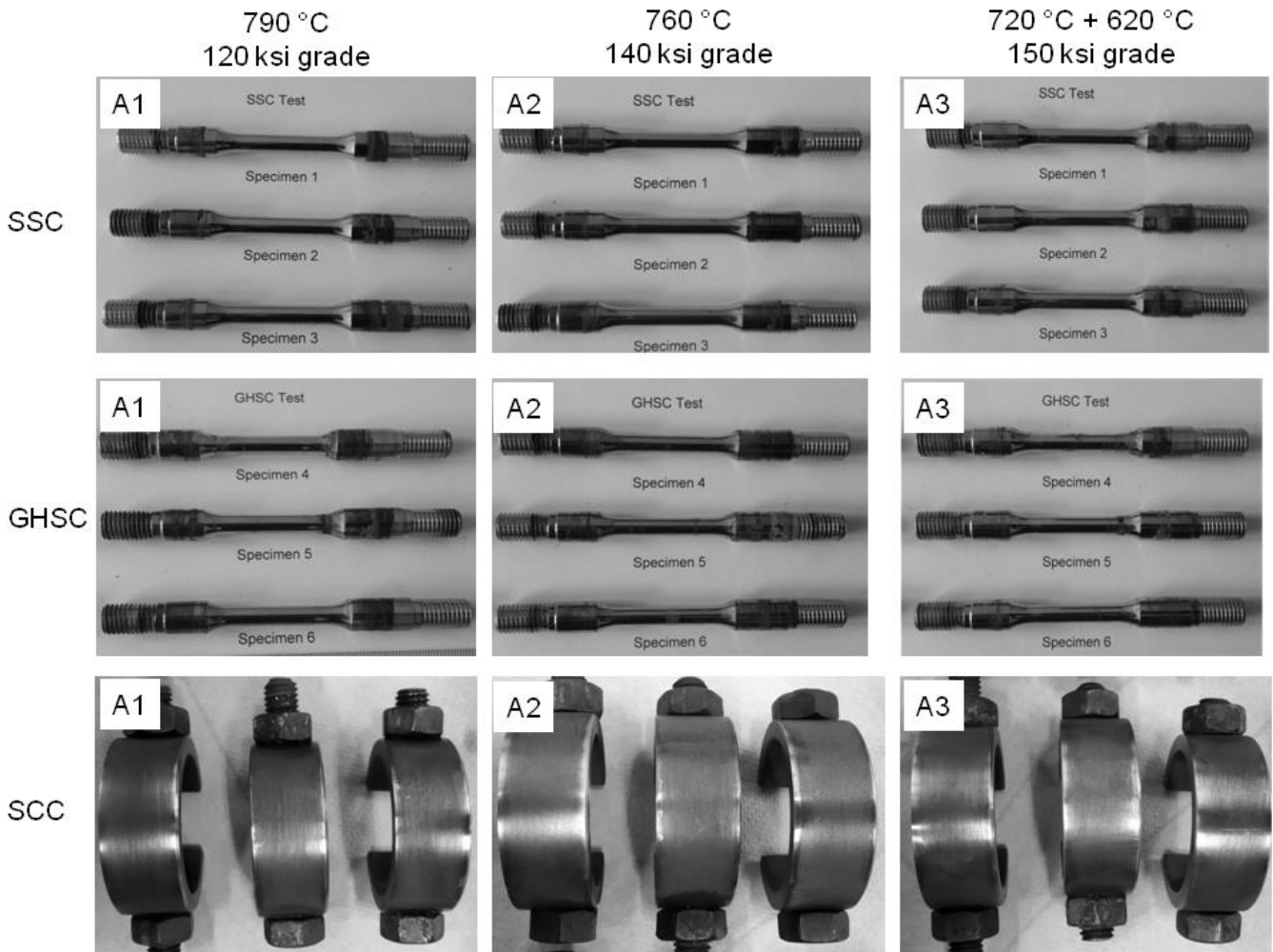


Figure 4: SSC specimens after test according to NACE TM0177 Method A for 30 d; GHSC specimens after test according to NACE TM0177 Method A for 30 d; SCC specimens after test according to NACE TM0177 Method C for 90 d at Level VII environmental conditions and stress level corresponding to 100 % AYS at test temperature.

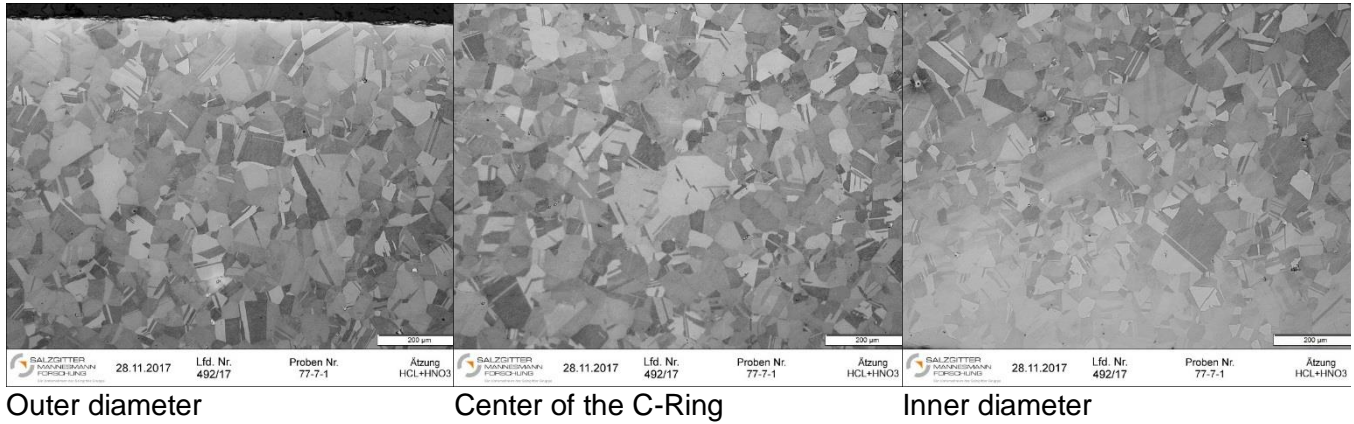


Figure 5: Microstructure of sample C3 after the SCC test for 180days at Level VII environmental conditions and stress level corresponding to 100% AYS at test temperature.

Hydrogen Embrittlement (HE) Resistance

The susceptibility to HE of Alloy UNS N07718 was evaluated by means of SSRT testing. From comparison of the ductility parameters determined in the test environment with those determined in the control environment, ductility ratios (elongation at failure and reduction-in-area ratio) were calculated and are shown in **Figure 6**. Values near 100 % generally indicate high resistance to environmental cracking. Moreover, a value of 45 % for the elongation at failure ratio is regarded as threshold level for classifying precipitation-hardened nickel base alloys with respect to their HE susceptibility.²⁷ Lower values generally indicate increased sensitivity to HE. All material grades of Alloy UNS N07718 tested here showed corresponding elongation at failure ratios well above 45 %, assuming good resistance to HE. No significant differences for the HE resistance between the 150 ksi grade and the lower yield strength material grades of Alloy UNS N07718 were observed. **Figure 7** shows a correlation between hardness (HRC) and ductility ratios observed in SSRT testing. The detailed SSRT test results, including reduction-in-area, elongation at failure, time to failure and maximum force are summarized in **Table 8**. Increasing hardness is found not to affect HE resistance of Alloy UNS N07718 material grades tested here.

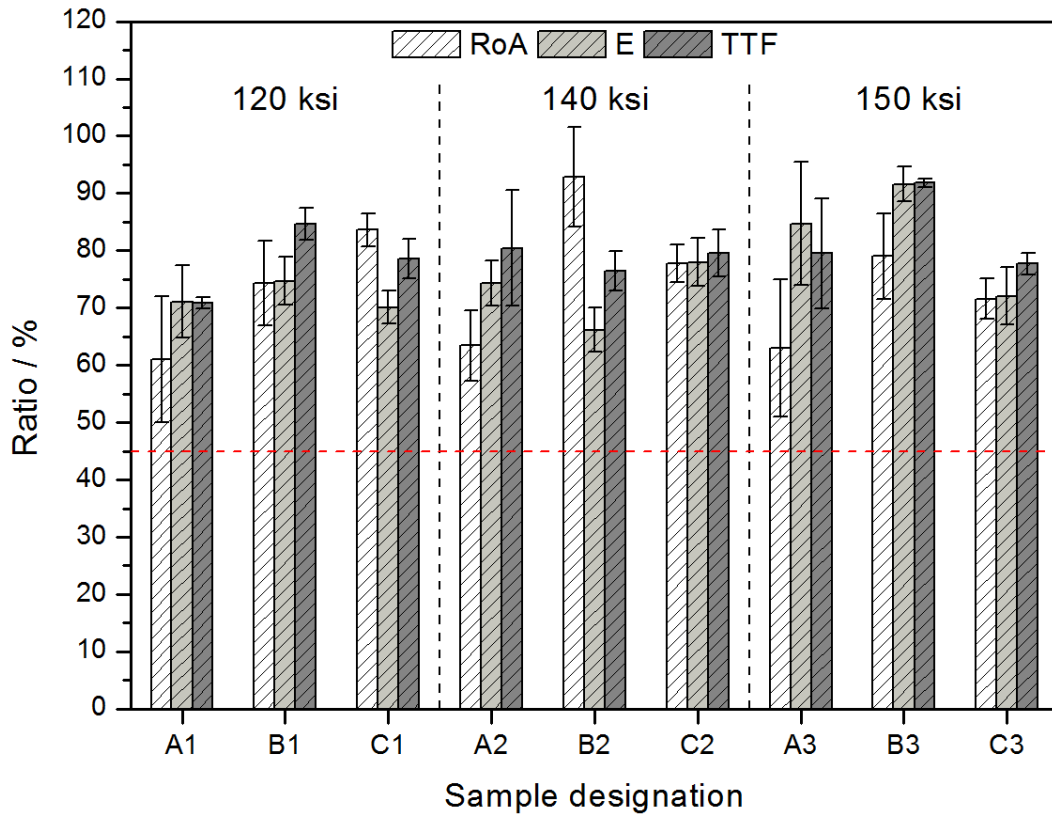


Figure 6: SSRT results for evaluating HE resistance of Alloy 718 grades.
 (RoA: reduction of area, E: elongation, TTF: time to failure)

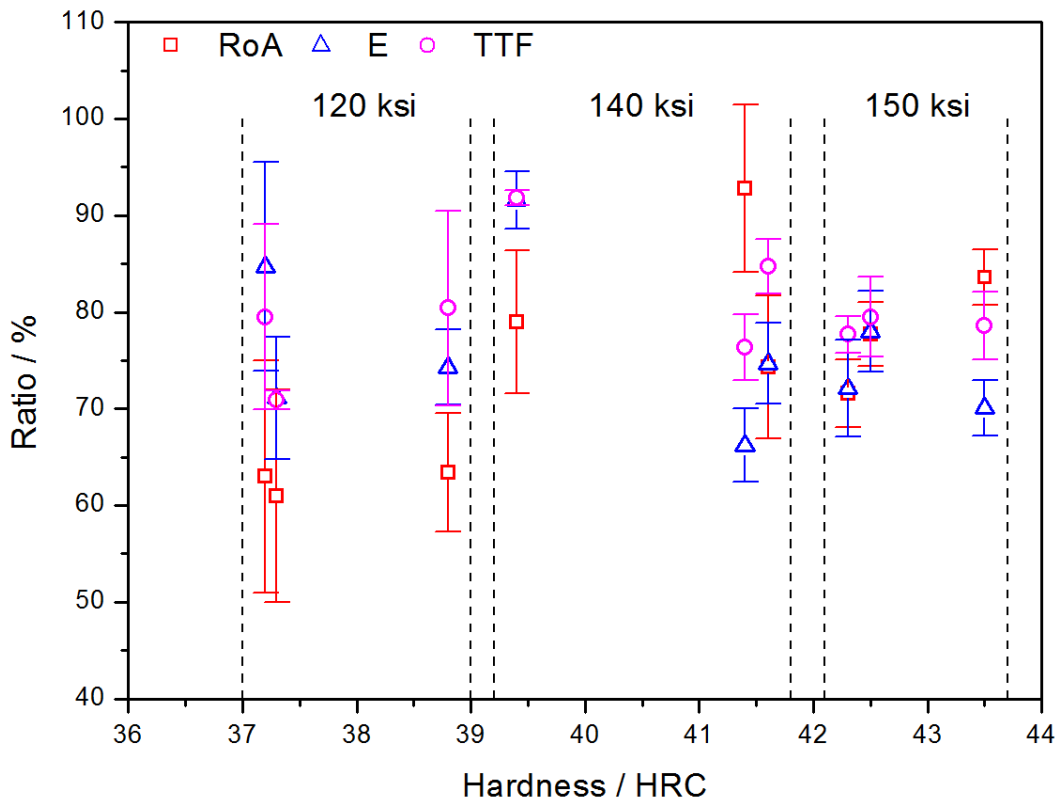


Figure 7: Correlation between hardness and ductility ratios observed from SSRT testing.
 (RoA: reduction of area, E: elongation, TTF: time to failure)

Table 8
Hydrogen Embrittlement SSRT results.

Sample n°	Test parameters	Reduction of Area		Elongation		Time to failure			Tensile strength	
		[%]	Ratio [%]	[%]	Ratio [%]	min	[h]	Ratio [%]	kN	Ratio [%]
A1	inert	55.2		25.8		5229	87.2		13.5	
	polarized	25.0	45.4	20.4	79.1	3751	62.5	71.7	13.3	98.3
	polarized	37.7	68.2	16.4	63.6	3633	60.6	69.5	15.5	114.4
	polarized	38.3	69.4	18.3	70.7	3743	62.4	71.6	15.9	117.4
	Average (pol.)	33.7	61.0	18.4	71.1	3709	61.8	70.9	14.9	110.0
A2	inert	59.5		31.3		4779	79.7		13.7	
	polarized	36.3	61.1	22.2	70.9	3196	53.3	66.9	14.7	107.4
	polarized	34.1	57.4	25.0	79.8	3971	66.2	83.1	13.5	98.5
	polarized	42.6	71.7	22.6	72.2	4355	72.6	91.1	13.2	96.3
	Average	37.7	63.4	23.2	74.3	3841	64.0	80.4	13.8	100.7
A3	inert	66.2		25.5		4809	80.2		15.6	
	polarized	40.3	60.9	22.4	87.7	3966	66.1	82.5	16.3	104.2
	polarized	32.7	49.4	17.9	70.2	3205	53.4	66.6	16.1	103.0
	polarized	52.1	78.6	24.5	96.2	4304	71.7	89.5	14.3	91.3
	Average	41.7	63.0	21.6	84.7	3825	63.8	79.5	15.5	99.5
B1	inert	68.0		24.8		5283	88.1		13.0	
	polarized	47.5	69.9	19.1	77.0	4370	72.8	82.7	13.9	106.9
	polarized	50.0	73.5	17.1	69.0	4370	72.8	82.7	13.1	100.8
	polarized	53.9	79.3	19.4	78.2	4680	78.0	88.6	13.1	100.8
	Average	50.5	74.2	18.5	74.7	4473	74.6	84.7	13.4	102.8
B2	inert	63.2		26.7		5560	92.7		11.0	
	polarized	65.1	103.0	18.8	70.4	4447	74.1	80.0	14.0	127.3
	polarized	59.1	93.5	18.0	67.4	4310	71.8	77.5	13.4	121.8
	polarized	51.6	81.6	16.3	61.0	3991	66.5	71.8	13.9	126.4
	Average	58.6	92.7	17.7	66.3	4249	70.8	76.4	13.8	125.2
B3	inert	76.6		18.6		4320	72.0		12.9	
	polarized	66.1	86.3	17.8	95.7	3970	66.2	91.9	13.2	102.3
	polarized	62.8	82.0	16.5	88.7	3923	65.4	90.8	13.3	103.1
	polarized	52.8	68.9	16.9	90.9	4006	66.8	92.7	13.5	104.7
	Average	60.6	79.1	17.1	91.8	3966	66.1	91.8	13.3	103.4
C1	inert	66.7		22.5		5029	83.8		14.2	
	polarized	58.1	87.1	16.7	74.2	4203	70.1	83.6	14.0	98.6
	polarized	53.3	79.9	15.2	67.6	3823	63.7	76.0	13.7	96.5
	polarized	55.8	83.7	15.4	68.4	3826	63.8	76.1	13.3	93.7
	Average	55.7	83.6	15.8	70.1	3951	65.8	78.6	13.7	96.2
C2	inert	55.2		21.6		5218	87.0		14.4	
	polarized	44.6	80.8	18.0	83.3	4243	70.7	81.3	13.5	93.8
	polarized	43.7	79.2	16.8	77.8	4347	72.5	83.3	14.4	100.0
	polarized	40.4	73.2	15.7	72.7	3853	64.2	73.8	13.4	93.1
	Average	42.9	77.7	16.8	77.9	4148	69.1	79.5	13.8	95.6
C3	inert	72.2		21.0		4737	79.0		13.7	
	polarized	54.0	74.8	14.4	68.6	3699	61.7	78.1	13.5	98.5
	polarized	48.2	66.8	16.6	79.0	3563	59.4	75.2	14.2	103.6
	polarized	52.8	73.1	14.4	68.6	3776	62.9	79.7	13.7	100.0
	Average	51.7	71.6	15.1	72.1	3679	61.3	77.7	13.8	100.7

CONCLUSIONS

The results of studying the effect of heat treatment on the properties of alloy UNS N07718 demonstrate that an increase of strength up to a 150 ksi yield strength grade has no negative effect on the resistance to corrosion (SSC, SCC, GHSC) and hydrogen embrittlement under the given heat treatment parameters. From the investigations, aiming at correlating mechanical properties (strength, hardness) and corrosion resistance, the following conclusions can be drawn:

- Mechanical properties of alloy UNS N07718 were successfully adjusted to achieve a strength level of 150 ksi using a two-step age hardening process.
- As shown by SEM analysis, decreasing age hardening temperature led to the formation of finer gamma” particles in the microstructure of alloy UNS N07718, which are responsible for an increase of strength and hardness levels. The duration of age hardening which has also an effect on strength was not investigated within this study.
- A correlation between strength level and hardness was verified for alloy UNS N07718.
- No negative impact of hardness values well above 40 HRC was found on the SSC, SCC or GHSC resistance of the tested alloy UNS N07718.
- Based on ductility parameters obtained from SSRT test data, no hydrogen embrittlement susceptibility of the tested grades of alloy UNS N07718 was detected.

The investigations confirmed the excellent corrosion resistance of UNS N07718 in oil and gas applications regardless of the strength or hardness level. Higher strength material of UNS N07718 showed as good HE resistance as the standard grades of this alloy. Other factors affecting the HE susceptibility were not investigated within this study.

ACKNOWLEDGEMENTS

The authors would like to thank Dr. H. Schlerkmann (Salzgitter Mannesmann Forschung GmbH) and Dr. B. Gehrmann (VDM Metals International GmbH) for support and technical discussions.

REFERENCES

1. API Standard 6ACRA, First Edition (August 2015), “Age-hardened Nickel-based Alloys for Oil and Gas Drilling and Production Equipment” (Washington, NW: API Publishing Services).
2. ANSI⁽⁶⁾ NACE TM0177-2016 (latest revision), “Laboratory testing of metals for resistance to sulfide stress cracking and stress corrosion cracking in H₂S environment” (Houston, TX: NACE International).
3. ANSI/NACE MR0175/ISO 15156-1-3:2015 (latest revision), “Petroleum, petrochemical, and natural gas industries – Materials for use in H₂S-containing environments in oil and gas production – Part 1 and 3” (Houston, TX: NACE International).
4. U. Heubner, J. Klöwer and 5 co-authors: *Nickel Alloys and high-alloyed special stainless steels*, 4th edition (Renningen, Germany: Expert-Verlag, 2012).
5. D. E. Williams, R. N. Tuttle, “ISO 15156/NACE MR0175 – a new international Standard for metallic Materials for Use in Oil and Gas Production in Sour Environment,” CORROSION/2003, paper no. 03090 (Houston, TX: NACE 2003).
6. S. A. McCoy, S. K. Mannan, C. S. Tassen, D. Maitra, J. R. Crum, “Investigation of the effect of Hydrogen on High Strength Precipitation Hardened Nickel alloys for O&G service,” CORROSION/2015, paper no. 5911 (Houston, TX: NACE, 2015).
7. R. B. Bhavsar, A. Collins, S. Silverman, “Use of Alloy 718 and 725 in Oil and Gas Industry,” Superalloys 718, 625, 706 and Various Derivates, 9, TX: The Minerals, Metals & Materials Society, 2001).

⁽⁶⁾ Approved American National Standard (ANSI)

8. C. Wang, R. Li, "Effect of double aging treatment in structure in Inconel 718 alloy," *Journal of Materials Science* 39 (2004): 2593-2595.
9. A., Devaux, I. Nazé, R. Molins, A. Pineau, "Gamma double prime precipitation kinetic of Alloy 718," *Materials Science and Engineering A* 486 (2008): 117-122.
10. B. Kagay, K. Findley, S. Corywell, A. Nissan, "Slow Strain Rate and Step Load Hydrogen Embrittlement Testing of UNS N07718," *CORROSION/2016*, paper no. 7861 (Houston, TX: NACE, 2016).
11. C. Silva, M. Song, K. Leonard, W. Wang, G. was, J. Busby, "Characterization of alloy 718 subjected to different thermomechanical treatments," *Materials Science & Engineering A* 691 (2017): 195-202.
12. L. Liu, K. Tanaka, A. Hirose, K. F. Kobayashi, "Effects of precipitation phases on the hydrogen embrittlement sensitivity of Inconel 718," *Science and Technology of Advanced Materials* 3 (2002): 335-344.
13. J. Kloewer, H. Sarmiento-Klapper, O. Gosheva, Z. Tarzimoghadam, "Effect of Microstructural Particularities on the Corrosion Resistance of Nickel Alloy UNS N07718 – What really makes the Difference," *CORROSION/2017*, paper no. 9068 (Houston, TX: NACE, 2017).
14. L. Fournier, D. Delafosse, T. Magnin, "Cathodic hydrogen embrittlement in alloy 718," *Materials and Science and Engineering A* 269 (1999): 111-119.
15. M. C. Rezende, L. S. Araujo, S. B. Gabriel, D. S. dos Santos, L. H. de Almeida, "Hydrogen embrittlement in nickel-based superalloy 718: Relationship between $\gamma' + \gamma''$ precipitation and the fracture mode," *International Journal of Hydrogen Energy* 40 (2015): 17075-17083.
16. S. Chen, M. Zhao, L. Rong, "Role of γ' characteristic on the hydrogen embrittlement susceptibility of Fe-Ni-Cr alloys," *Corrosion Science* 101 (2015): 75-83.
17. Z. Tarzimoghadam, "Hydrogen-assisted failure in Ni-base alloys UNS N07718", *CORROSION/2016*, paper no. 7459 (Houston, TX: NACE, 2016).
18. O. Gosheva, "Impact of microstructure on hydrogen solubility and diffusivity in UNS N07718", *CORROSION/2016*, paper no. 7267 (Houston, TX: NACE, 2016).
19. B. Kagay, K. Findley, S. Coryell, A.B. Nissan, "Effects of alloy 718 microstructure on hydrogen embrittlement susceptibility for oil and gas environments", *Material Science and Technology Vol. 32, No 7-8* (2016): 697-707.
20. W. Huang, W. Sun, A. Samson, D. Muise, „Investigation of Hydrogen Embrittlement Susceptibility of Precipitation hardened Nickel Alloys under Cathodic Protection Condition“, *CORROSION/2014*, paper no. 4248 (Houston, TX: NACE, 2014).
21. ASTM E112-13, "Standard test Methods for Determining Average Grain Size" (West Conshohocken, PA: ASTM International).
22. ISO 6892-1:2009-12, "Metallische Werkstoffe – Zugversuch – Teil 1: Prüfverfahren bei Raumtemperatur".
23. ISO 6892-2:2011-05, "Metallische Werkstoffe – Zugversuch – Teil 2: Prüfverfahren bei erhöhter Temperatur".
24. ISO 6508-1:2016-12, „Metallische Werkstoffe – Härteprüfung nach Rockwell – Teil 1: Prüfverfahren“.
25. ISO 148-1:2011-01, "Metallische Werkstoffe – Kerbschlagbiegeversuch nach Charpy – Teil 1: Prüfverfahren".
26. NACE TM0198-2016, "Slow Strain Rate Test Method for Screening Corrosion-Resistant Alloys (CRAs) for Stress Corrosion Cracking in Sour Oilfield Service", (Houston, TX: NACE International).
27. L. Feroni, "Hydrogen Embrittlement Susceptibility of Precipitation Hardened Ni-Alloys", *CORROSION/2014*, paper no. 3948 (Houston, TX: NACE, 2014).